Morphology, Thermal, and Mechanical Properties of Acrylonitrile–Butadiene–Styrene/Carbon Black Composites

A. Shenavar, F. Abbasi

Research Center for Polymeric Materials, Sahand University of Technology, Tabriz, Iran

Received 26 August 2006; accepted 8 January 2007
DOI 10.1002/app.26219
Published online 26 April 2007 in Wiley InterScience (www.interscience.wiley.com).

ABSTRACT: Acrylonitrile–butadiene–styrene (ABS) polymers are susceptible to degradation that increases the yellowness of the polymer, distorts the surface glossy, and affects the mechanical properties. One way to protect ABS against degradation is the addition of carbon black (CB) that can act as a stabilizer. In this work, CB was dispersed in ABS through melt-compounding. Electron microscopy was used to study the morphology of the filled- and unfilled-ABS, and revealed that the CB particles/aggregates were distributed within the styrene–acrylonitrile (SAN) phase and around the PB phase. The results of the Fourier transform infrared spectroscopy showed that upon processing of ABS, crosslinking in the polybutadiene (PB) phase was the governing degradation mechanism. Increasing the CB content resulted in increasing the heat stability of the ABS/CB compounds, which was confirmed by thermogravimetric analysis. The DTA results showed that the PB degradation peak occurring at about 395°C was disappeared by addition of CB. Impact strength test was performed to study the effect of CB on the toughness of ABS. Impact strength was reduced with increasing CB loading. © 2007 Wiley Periodicals, Inc. J Appl Polym Sci 105: 2236–2244, 2007

Key words: ABS; carbon black; composite; morphology; thermal behavior

INTRODUCTION

Acrylonitrile–butadiene–styrene (ABS) terpolymer is an engineering plastic used widely in industry owing to its good mechanical and processing properties. ABS is usually filled with rubber particles[1] or rigid inorganic particles (RIP), such as calcium carbonate ($CaCO_3$),[2] kaolin and glass bead,[3–5] talcum powder,[6] and carbon black,[7] to further enhance its strength, toughness, stiffness, thermal stability and also to reduce the production cost.

In the last three decades, the effects of filler content, filler size and size distribution, surface treatment of the filler on the tensile yield strength, impact strength, the modulus, the flexural strength, the interfacial adhesion between the matrix and fillers of the ABS and its blends and composites have been studied.[3–14]

Discoloration, distortion of the surface glossy, thermal degradation, oxidation, and photo-oxidation are the important disadvantages of ABS products during the processing, and applications at high temperature and outdoor conditions. Many studies have been directed toward understanding how chemical aging occurs in ABS and how its effects can be minimized. Gesner,[15] Alekseev et al.,[16] and Tiganis et al.[17] have shown that the thermo-oxidation of ABS occurs in the polybutadiene (PB) phase of the resin. The results of another study regarding degradation of ABS during processing showed that PB was the least stable component toward thermal oxidation.[18]

Carbon blacks (CBs) consist of aggregates, which are composed of partially coalesced primary particles. The smaller the primary particle, the larger is the surface area. However, a high surface area black is hard to disperse and achieve its full potential in color and other physical properties. Yu et al.[7] studied the color, viscosity, and Izod impact properties of ABS filled with different structure and surface area CBs. ABS was used to make masterbatch and the masterbatch was then diluted with ABS to afford 1% CB loading. The viscosity increased and the impact strength decreased with increasing the CB loading in masterbatch. The impact strength decreased with increasing structure and surface area of filler.[7]

In this work, the ABS/CB composites were prepared and studied in terms of thermal properties and stability. Morphology and distribution of the CB particles within the ABS components were also investigated.

EXPERIMENTAL

Materials

The ABS resin (ABS SD 0150) and styrene–acrylonitrile (SAN APO) copolymer were made by TPC

Correspondence to: Dr. F. Abbasi (f.abbasi@sut.ac.ir).

Journal of Applied Polymer Science, Vol. 105, 2236–2244 (2007)

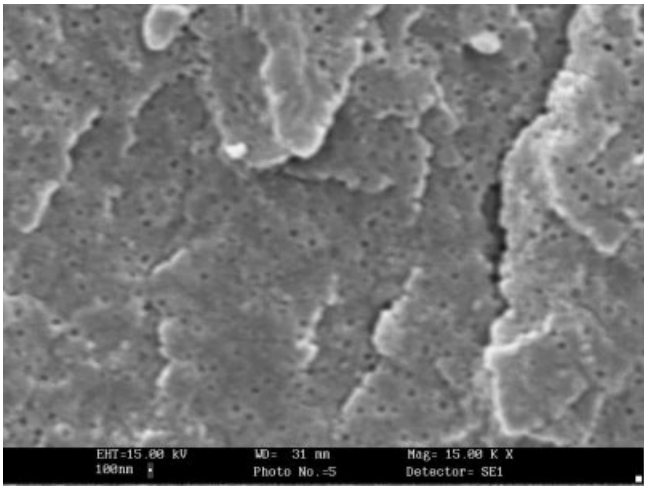

Figure 1 SEM micrograph obtained from freeze fractured surface of etched ABS.

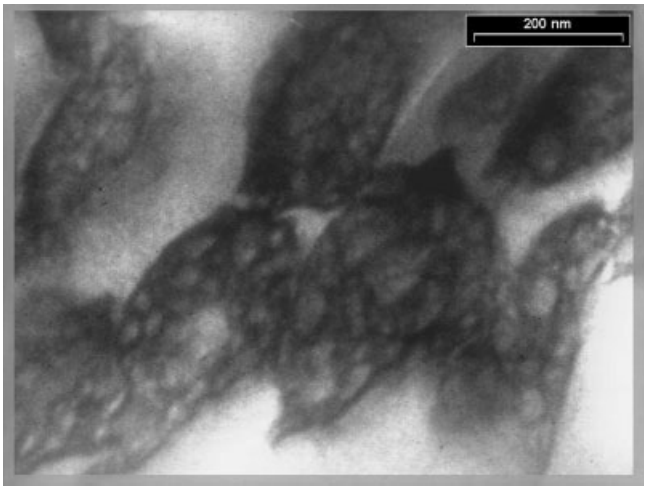

Figure 3 Transmission electron micrograph of OsO_4-stained ABS.

(Tabriz, Iran). The solid-state density and melt flow index (according to ASTM D1238) of the resin were 1.05 g/cm^3 and 1.7 g/10min, respectively. CB powder (N330) was obtained from Iran Carbon Company (Ahvaz, Iran). The mean diameter of the particles and aggregates sizes were 46 and 146 nm, respectively, and its surface area was 80 m^2/g. Tetrahydrofuran (THF), CrO_3, H_2SO_4, and OsO_4 were supplied by Merck (Darmstadt, Germany).

Methods

Sample preparation

ABS/CB compounds were prepared by melt-mixing in a Brabender DSE 25 twin-screw extruder ($L/D = 30$, corotating, intermeshing) (Germany). The six heating zones were set at 220, 220, 220, 220, 220, and 230°C. To study the effects of the compounding conditions

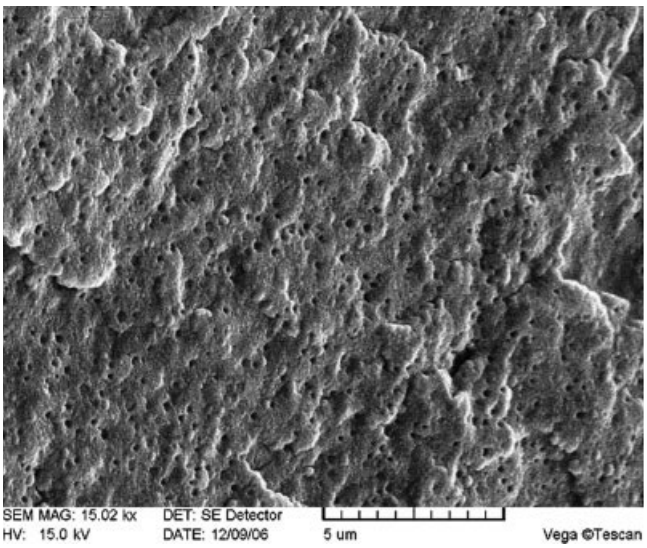

Figure 2 SEM micrograph obtained from freeze fractured surface of ABS.

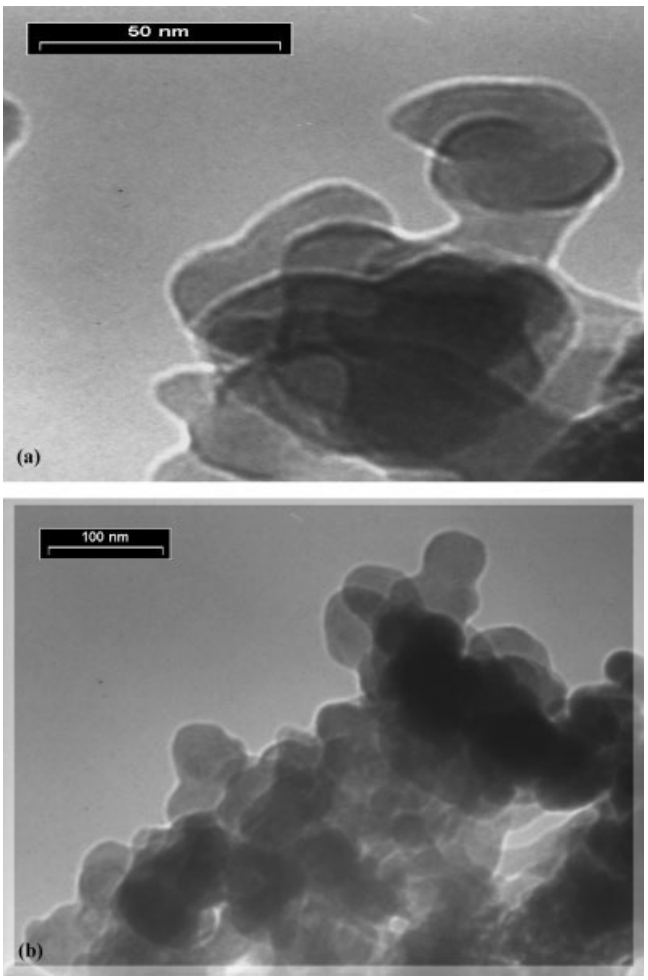

Figure 4 Transmission electron micrograph of CB, indicating (a) the aggregates and (b) the agglomerates.

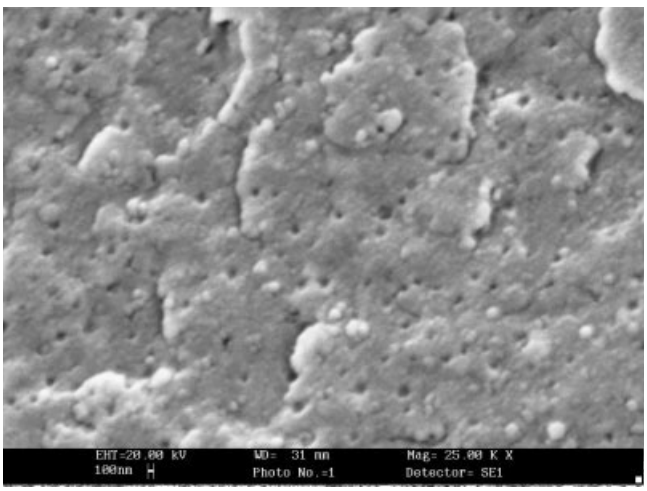

Figure 5 SEM micrograph obtained from freeze fractured surface of the etched ABS/CB compound having 2 wt % CB.

on the properties of unfilled ABS, this material was processed under the conditions same as the ABS/CB compounds in twin-screw extruder. The extruded strands were quenched immediately in water at room temperature and chopped into granules. The obtained granules were dried at 80°C for 16 h.

The specimens for impact tests were molded using an Engel injection molding machine (Austria) at injection temperatures varying from 170 to 220°C.

Apparatus and methodology

Morphology of the freeze fractured surfaces and fracture surfaces obtained from impact tests of the samples were studied using scanning electron microscopy (SEM) with a scanning electron microscope (LEO 440I, UK). Transmission electron microscopy (TEM) of ABS and its composites was carried out by a Philips CM200 FEG (Germany) electron microscope. The TEM specimens were prepared according to the following procedure: The sample surface was first smoothed using a glass knife, followed by staining in the vapor of 2 wt % OsO_4 aqueous solution for 48 h. Staining helps to increase the brittleness of the rubber particles and to enhance the contrast between the rubber particle and the matrix. The stained samples were microtomed using a diamond knife at ambient temperature to obtain thin sections of $\sim$ 50 nm in thickness.

For SEM analysis, the rubber phase was etched in a solution of 320 g/L CrO_3 with 400 g/L H_2SO_4 for a period of 5 min at 63°C.

The impact tests were carried out in Charpy mode according to ASTM D256 using a Roell Amsler-RKP300 (Germany) machine. For each composition, four specimens were tested and the average impact strength and standard deviation were reported.

Fourier transform infrared (FTIR) spectroscopy was used to study the processing-induced degradation and chemical changes in the microstructure of ABS. To investigate the effect of the processing on the degradation of polymer, IR spectra of ABS, processed ABS, and ABS/CB compounds were obtained with a Unicam Mattson 1000 FTIR (UK).

The thermal properties of the samples were examined by Perkin–Elmer Pyris TG/DTA thermogravimeter (Japan) with a heating rate of 20°C/min and different purge gases.

RESULTS AND DISCUSSION

Morphological studies

ABS terpolymers contain rubber particles embedded in a styrene–acrylonitrile copolymer (SAN) matrix. Figures 1 and 2 show the SEM micrographs obtained from freeze fractured surfaces of unfilled ABS with and without etching. The black holes in Figure 1 are attributed to the etched PB particles. On the other hand, the black holes in Figure 2 indicate that the holes remained from pulling out of the PB particles. The white particles in Figure 2 indicate the PB particles remained on the broken surface.

The morphology of the rubber domains stained by OsO_4 can be seen in TEM micrograph (Fig. 3). This figure indicates the well-known morphology of the phase-within-a-phase-within-a-phase in which SAN forms the continuous phase and dispersed rubber particles contain the occluded SAN.

The micrographs indicating CB aggregates and agglomerates are shown in Figures 4(a,b), respectively. The aggregates are composed of primary particles having a diameter varying from 30 to 50 nm and the agglomerates are composed of the aggregates.

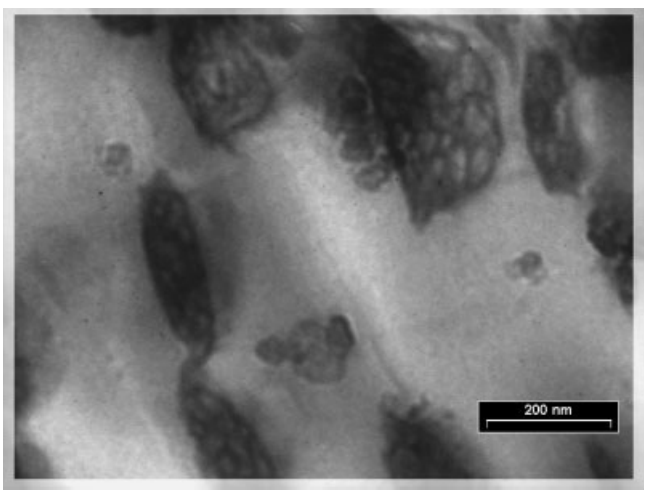

Figure 6 Transmission electron micrograph of an ABS/CB compound having 2 wt % CB.

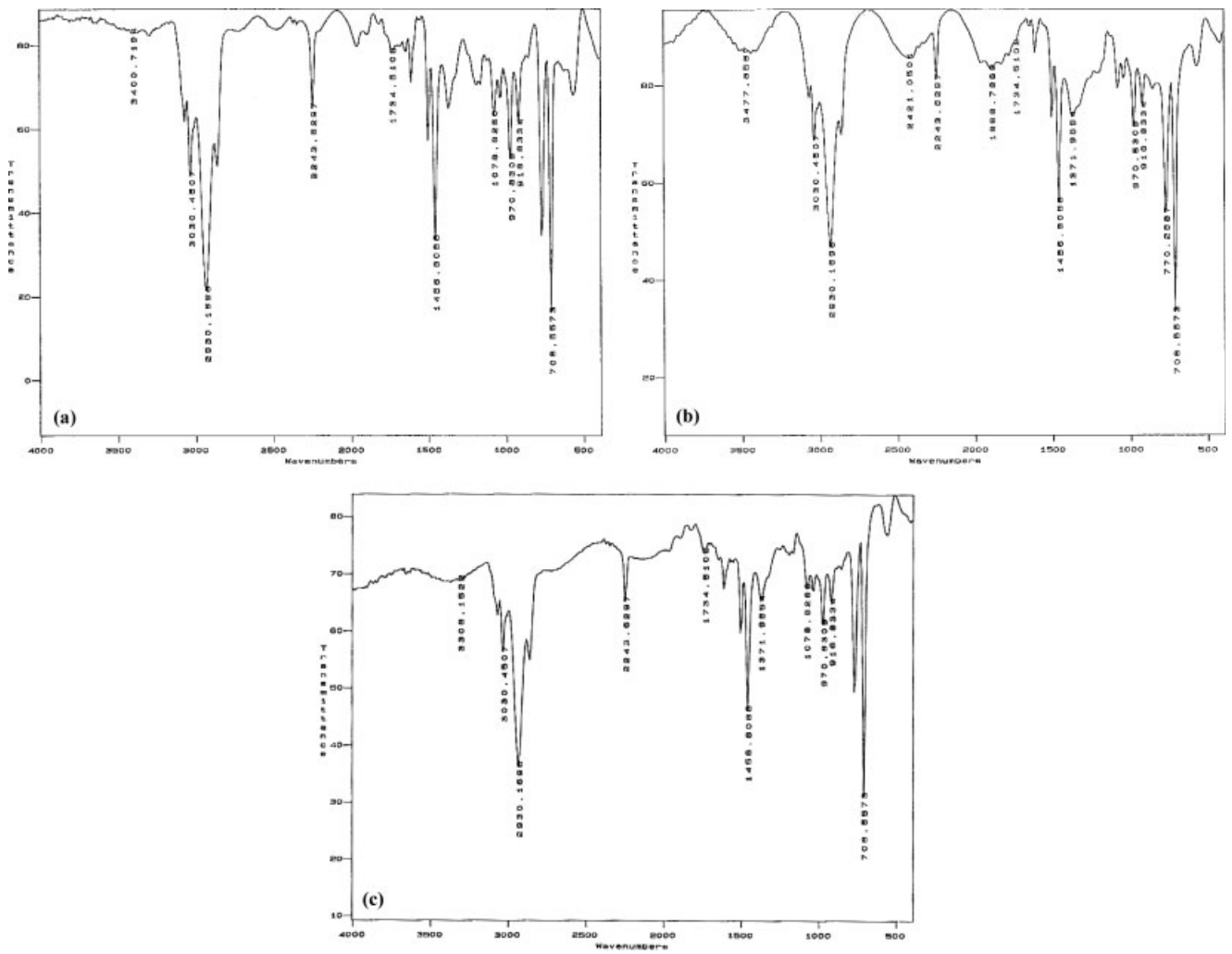

Figure 7 FTIR spectra of (a) ABS, (b) processed ABS, and (c) ABS/CB compound having 2 wt % CB.

The SEM micrograph of an ABS/CB compound having 2 wt % CB is shown in Figure 5. With comparing the micrographs of Figures 1 and 5, it can be concluded that the white points in Figure 5 belong to CB particles and aggregates.

Figure 6 indicates a TEM cross section stained with OsO_4 to distinguish between the PB and SAN phases. This method also allows the relative positions of the PB and CB particles to be studied. As shown, the CB aggregates and particles exist in the SAN phase and around the PB particles, but, due to the same color of the CB and PB particles in TEM, it is difficult to investigate the presence of the CB particles within the rubber phase. However, the crosslinked structure of PB particles may prevent incorporation of the CB particles into the PB phase.

Heat stability

FTIR spectroscopy

While the loss of mechanical properties in ABS is often attributed to thermo-oxidative degradation in the PB phase, thermo-oxidative degradation and physical aging can also occur in the SAN phase.[15–17]

The FTIR spectra for the virgin and processed ABS and ABS/CB compounds are shown in Figure 7. The absorption bands occurring at 970 and 916 cm^{-1} correspond to the trans C=C unsaturation (vinyl) in PB, and the 1,2-butadiene terminal vinyl C—H band, respectively. The results show a significant decrease in the intensities of absorbances at 970 and 916 cm^{-1}

TABLE I
Reduction in the Intensity of the Absorption Bands at 970 and 916 cm^{-1}

Reduction in the intensity of the absorption band (%)[a]	Processed ABS	ABS/CB with 2 wt % CB
$\left(\frac{D_{970}}{D_{708}}\right)_{\text{sample}} \Big/ \left(\frac{D_{970}}{D_{708}}\right)_{\text{ABS}}$	18	8
$\left(\frac{D_{916}}{D_{708}}\right)_{\text{sample}} \Big/ \left(\frac{D_{916}}{D_{708}}\right)_{\text{ABS}}$	21	13

[a] D_{970} means the height of the absorbance peak at 970 cm^{-1} from baseline.

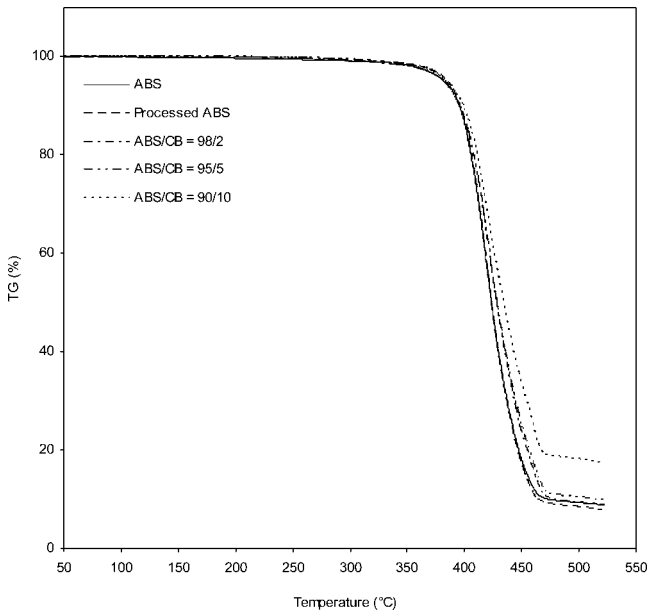

Figure 8 TGA thermograms for ABS and ABS/CB compounds in nitrogen.

for ABS/CB compounds (Table I), indicating chemical changes in the PB microstructure, which can be probably be attributed to chain scission and crosslinking. It has been reported that degradation of the PB phase at the surface forms hydroperoxide species, as indicated by the carbonyl (1724 cm^{-1}) and hydroxyl (3473 cm^{-1}) absorbances in the spectrum,[15–17,19,20] but the lack of oxygen in the bulk of polymer in mixing conditions can reduce these effects. The quantitative analysis of the obtained spectra was carried out using the 708 cm^{-1} absorption band corresponding to the out-of-phase bending vibration of the C—H band of benzene ring, which remains unchanged during processing.

Thermal degradation of the PB phase in ABS is initiated by hydrogen abstraction from carbon atoms in a α-position to unsaturated bonds. The abstraction generates radicals which, in the presence of oxygen, lead to the formation of carbonyl and hydroxyl products and without oxygen, lead to crosslinking of PB phase. Following a reaction scheme proposed by Shimada and Kabuki,[19] degradation products may decompose further to create various polymer radicals, which facilitate crosslinking and form degradation products such as polymer peroxides.

TG/DTA measurements

The results of TG measurements in nitrogen show that the onset temperature in mass change of the ABS/CB compounds is slightly increased with increasing the CB content (Fig. 8). By contrast, in oxygen as purging gas, the onset temperature is increased for the ABS/CB compound with 2 wt % CB. However, with further increasing the CB content, the onset temperature is decreased and reaches a minimum in 10 wt % of CB (Fig. 9). On the other hand, while the 50% weight loss temperature of the samples are improved with increasing the CB content, this temperature reaches its maximum value at 2 wt % of CB (Table II).

Increased onset temperature observed for the sample having 2 wt % CB may be due to the stabilizing effect of CB, thereby active groups present on the surface of CB particles react with created radicals. On the other hand, lower onset point of sample having 10 wt % CB on heating in oxygen can be attributed to distortion of the active groups on the surface of CB particles.

Suzuki et al. applied TGA/FTIR to investigate the degradation of ABS and they reported evolution temperatures of 340, 350, and 400°C for butadiene, styrene, and monomeric acrylonitrile, respectively.[21] The thermal degradation of PB was also studied by Chen and Qian. They reported two exotherms and two endotherms occurring at 383 and 546°C, and 440 and 512°C, respectively.[22] From DTA experiments [Fig. 10(a,b)], the glass transition temperature (T_g) of SAN occurred at about 110°C. The exothermic peak at about 230°C is attributed to the crosslinking in PB. The next peak at about 395°C relates to the isomerization of the PB and the peak occurring at about 420°C relates to the degradation of SAN. Other types of PB such as depolymerization occurred at higher temperatures.

As shown in Table III, the glass transition temperature is slowly increased with processing and in-

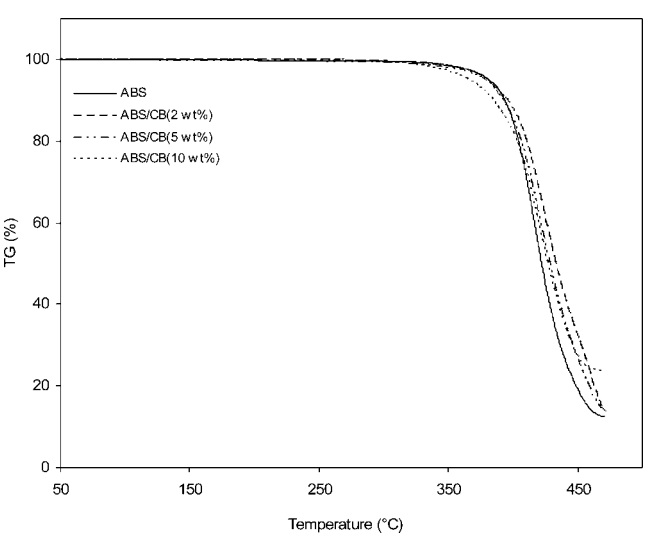

Figure 9 TGA thermograms for ABS and ABS/CB compounds in oxygen.

TABLE II
Initial Decomposition Temperature (IDT) and the 50% Weight Loss Temperature of ABS and Its Composites with CB

The 50% weight loss temperature (°C) in oxygen	IDT (°C) in oxygen	The 50% weight loss temperature (°C) in nitrogen	IDT (°C) in nitrogen	Sample
422	392.7	423.7	394.3	ABS
–	–	424.6	394.9	Processed ABS
428	397.3	425	394	ABS/CB (2 wt %)
426	391.4	426.7	396.3	ABS/CB (5 wt %)
426.3	389.3	430	394.8	ABS/CB (10 wt %)

creasing the CB content. However, processing decreases the crosslinking temperature of ABS [Fig. 10(a)]. Compared with processed ABS, this temperature is increased by increasing CB loading and reaches to about 228°C for ABS/CB compounds with 10 wt % CB. The third peak at about 395°C, which corresponds to the isomerization of PB, is disappeared for ABS/CB compounds [Fig. 10(c,d)].

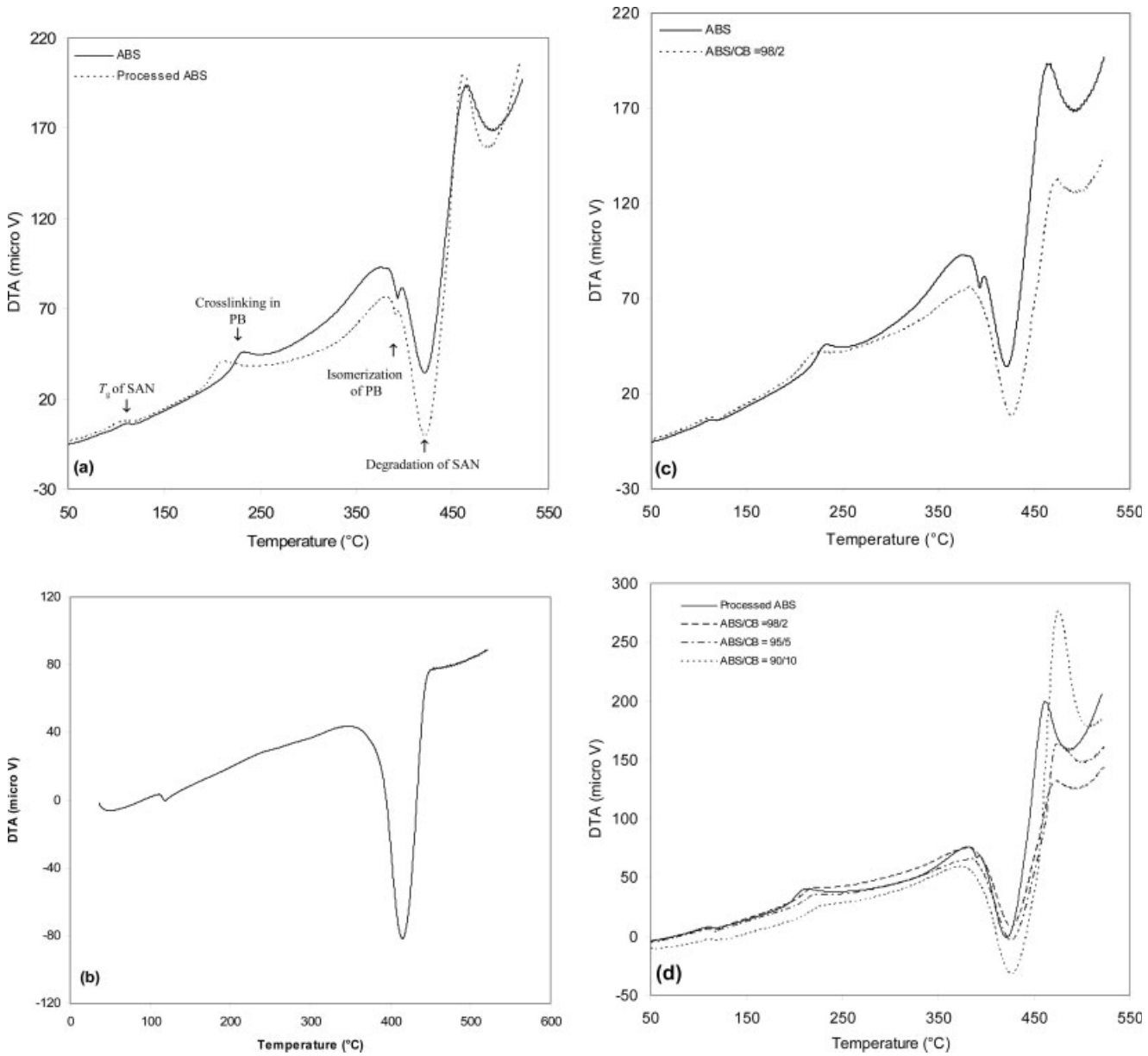

Figure 10 DTA thermograms for (a) ABS and processed ABS, (b) SAN, (c) virgin ABS and ABS/CB having 2 wt % CB, and (d) processed ABS and ABS/CB composites in nitrogen.

TABLE III
The Glass Transition and Crosslinking Temperatures of ABS and ABS/CB Composites Measured in Nitrogen

Crosslinking temperature (°C)	Glass transition temperature (°C)	Sample
229.5	113.3	ABS
209.1	114.5	Processed ABS
218.6	115.5	ABS/CB (2 wt %)
220.9	116	ABS/CB (5 wt %)
228	117.1	ABS/CB (10 wt %)

Impact strength

Figure 11 indicates the dependence of the Charpy notched impact strength of the ABS/CB composites on the filler content. As shown, the impact strength is decreased with processing and increasing the CB content.

Polymer degradation products form microstructural inconsistencies, which may act as stress concentration sites. Tiganis et al.[17] investigated the aging effect on the impact strength of ABS. The results showed that the impact strength of unnotched specimens was affected by thermal aging, compared with the notched specimens that are not affected by thermal aging. It is due to this fact that the degradation of the bulk polymer does not occur due to the limited oxygen diffusion. Thermal degradation of the SAN phase in ABS also occurs by physical aging and thermo-oxidative degradation, but has only a minor contribution to the deterioration of mechanical properties in ABS. Contrary to the aging, the processing-induced degradation occurred in the bulk of polymer and the notched impact strength is affected by processing.[17]

In ABS materials deformation mechanisms, both crazing and shear yielding may occur in the continuous SAN matrix. Figure 12 shows the SEM micrograph of a Charpy impact fractured specimen. This figure shows a smooth fracture surface with few cavities. Such a smooth fracture surface of impact specimens in which crazing was the predominant energy absorption mechanism was also reported by Jar et al.[23] for ABS toughened SMI (a copolymer of styrene, maleic-anhydride, and *N*-phenylmaleimide)/SAN blends. Lazzeri and Bucknall have proposed a model for rubber particle cavitation showing that the cavitation in the rubber particles cannot be formed by particles of less than 250 nm in diameter.[24]

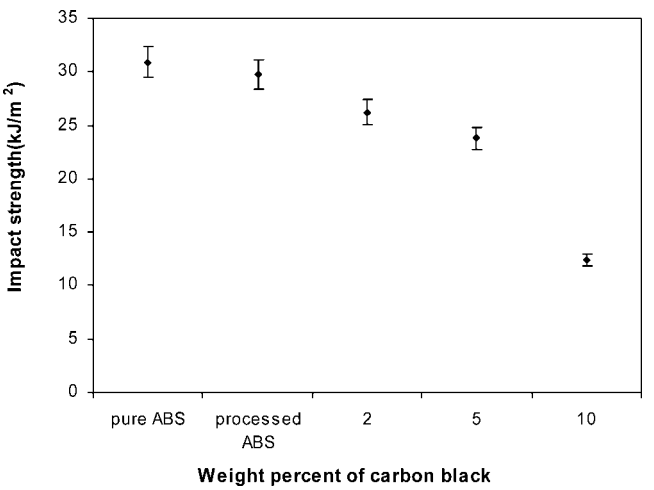

Figure 11 Impact strengths of the ABS/CB composites as a function of CB loading.

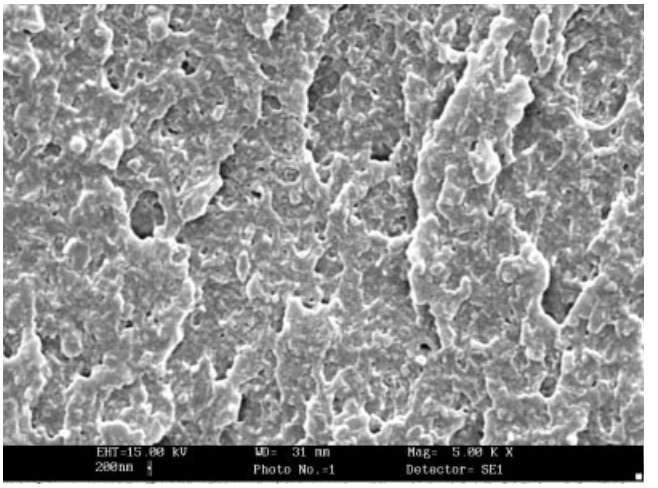

Figure 12 SEM micrograph of fracture surface of the Charpy impact specimen.

Even though unstable crack is the dominant crack mechanism, fracture surface analysis shows that stable crack propagation still occurs. Yanchun et al.[25–27] presented the schematic diagram showing the formation of various zones ahead of the crack tip, which include initial notch zone, shear deformation zone, crazing zone, and unstable fracture zone. The plastic zone consists of both crazing and shear deformation zones.

Figure 13 shows the SEM micrographs of the fracture surface and various zones ahead of the crack tip of ABS and ABS/CB composites. It can be seen that the stable fracture surface, zones (2) and (3), is decreased with increasing CB content. Contrary to the ABS, in which there is not an unstable fracture zone [Fig. 13(a)], in the ABS/CB composites, the semi brittle surface appeared when CB was added to the ABS [Fig. 13(b,c)]. With further increasing the CB content, it seems that the brittleness of the zone 4 has been greatly increased [Fig. 13(d)].

CONCLUSIONS

Because of the same color of CB and PB particles, it is difficult to detect the CB particles within the PB

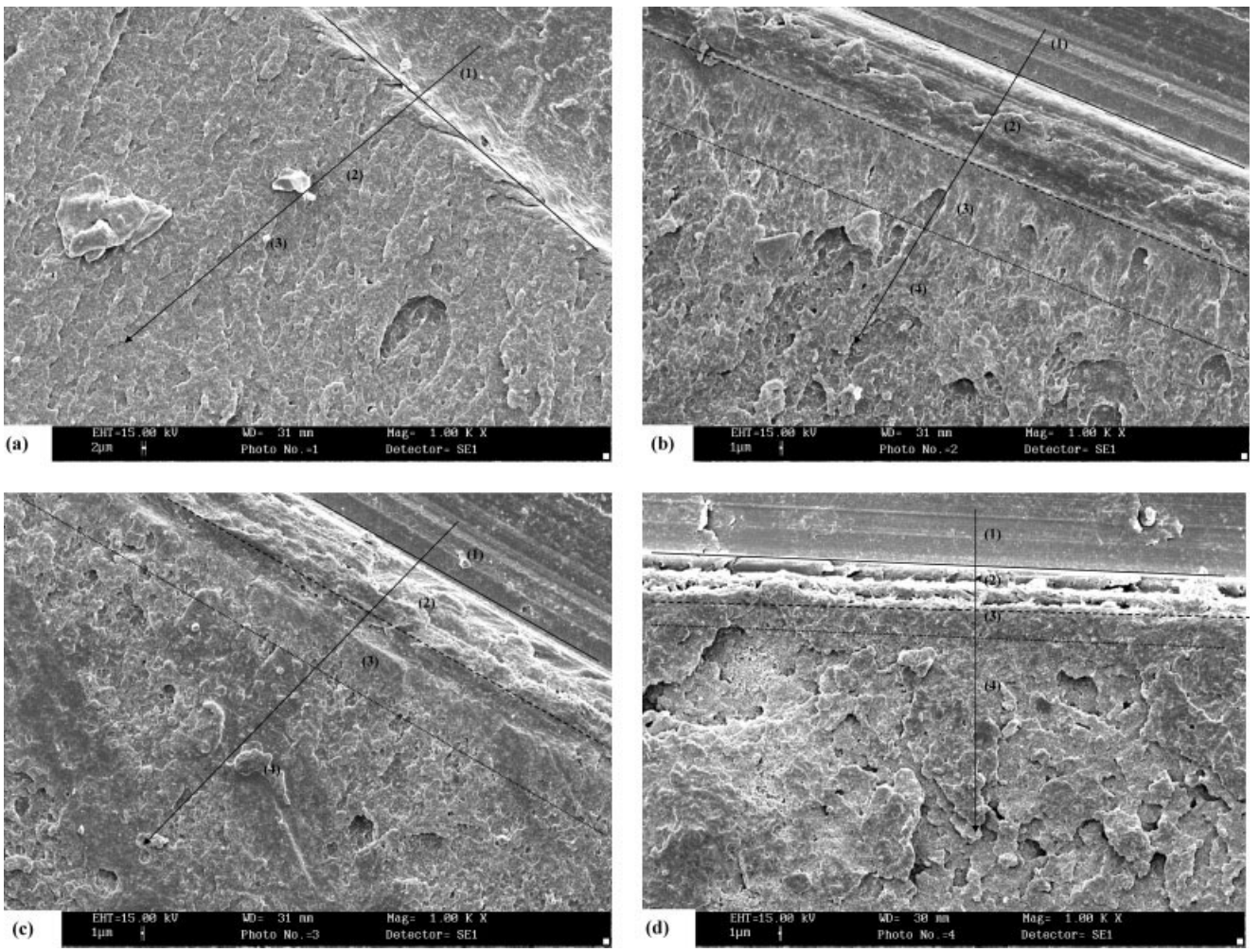

Figure 13 SEM micrograph of fracture surface of notched specimens, (a) ABS, (b) 2 wt %, (c) 5 wt %, and (d) 10 wt % of ABS/CB composites. The zones 1, 2, 3, and 4 indicate initial notch zone, shear deformation zone, crazing zone, and unstable fracture zone, respectively.

particles with electron microscopy. However, one can predict that the crosslinked structure of PB particles may prevent incorporation of CB into the PB phase, and the CB particles/aggregates are distributed in the SAN phase and around the PB particles.

The color of unfilled ABS changes to ''yellow to brown'' with processing and its glossy reduces. Thermo-oxidative degradation of the bulk polymer does not occur due to the limited oxygen diffusion. These results are in good agreement with FTIR analysis. Thermal degradation of PB phase in ABS initiated by hydrogen abstraction from carbon atoms in a α-position to unsaturated bonds. The abstraction generates radicals that lead to crosslinking in the PB phase.

Although degradation may occur in both SAN and PB phases, but crosslinking of PB phase is responsible for reduction in impact strength. The polymer degradation products form microstructural inconsistencies, which may act as stress concentration sites. Processed ABS and ABS/CB composites were found to have lower impact strength than ABS. Stable fracture surface was decreased with increasing CB contents.

The results of TG measurements in nitrogen showed that the onset temperature in mass change was slightly increased with increasing the CB content of the ABS. By contrast, the onset temperature in oxygen was increased for the ABS/CB compound with 2 wt % CB. However, with further increasing the CB content, the onset temperature was decreased and reached a minimum in 10 wt % of CB. On the other hand, while the 50% weight loss temperature of the samples are improved with increasing CB content, this temperature reaches its maximum value at 2 wt % of CB.

From DTA measurements, the peak at about 395°C relating to the degradation of PB was disappeared by addition of CB. The glass transition temperature of SAN was slowly increased with increasing CB

content. The crosslinking temperature of PB was decreased by processing and increased by increasing the CB content.

The authors thank Mr. A. Almasi at the Tabriz University for his kind assistance and SEM analysis. Most helpful discussions with Dr. M. K. Razavi at Sahand University of Technology are also gratefully acknowledged.

References

1. Grancio, M. R. Polym Eng Sci 1972, 12, 213.
2. Liang, J. Z. Polym Int 2002, 51, 1473.
3. Lavengood, R. E.; Nicolais, L.; Narkis, M. J Appl Polym Sci 1973, 17, 1173.
4. Liang, J. Z. J Elast Plast 2005, 37, 361.
5. Liang, J. Z. J Thermoplast Compos Mater 2005, 18, 407.
6. Bigg, D. M. Polym Compos 1987, 8, 115.
7. Yu, M. C.; Menashi, J.; Kaul, D. J. Proc ANTEC 1994, 40, 2524.
8. Turcsányi, B; Pukánszky, B.; Tüdös, F. J Mater Sci Lett 1988, 7, 160.
9. Narkis, M. J Appl Polym Sci 1976, 20, 1597.
10. Newmann, L. V.; Williams, J. G. J Mater Sci 1980, 15, 773.
11. Lu, M. L.; Lee, C. B.; Chang, F. C. Polym Eng Sci 1995, 35, 1433.
12. Yang, K.; Lee, S. H.; Oh, J. M. Polym Eng Sci 1999, 39, 1667.
13. Tjong, S. C.; Jiang, W. J Appl Polym Sci 1999, 73, 2985.
14. Tang, C. Y.; Chen, L. C.; Liang, J. Z.; Cheng, K. W. E.; Wong, T. L. J Reinfor Plast Compos 2002, 21, 1337.
15. Gesner, B. D. J Appl Polym Sci 1965, 9, 3701.
16. Alekseev, A. A.; Abdulrakhim, R. M.; Osipchik, V. S.; Kirichenko, E. A.; Chernyshoa, V. N. Int Polym Sci Technol 2003, 30, 18.
17. Tiganis, B. E.; Burn, L. S.; Davis, P.; Hill, A. J. Polym Degrad Stab 2002, 76, 425.
18. Blom, H.; Yeh, R.; Wojnarowski, R.; Ling, M. Thermochim Acta 2006, 442, 64.
19. Shimada, J.; Kabuki, K. J Appl Polym Sci 1968, 12, 665.
20. Wyzgoski, M. G. Polym Eng Sci 1976, 16, 265.
21. Suzuki, M.; Wilkie, C. A. Polym Degrad Stab 1995, 47, 217.
22. Chen, F.; Qian, J. Fuel Process Technol 2000, 67, 53.
23. Jar, P. Y. B.; Wu, R. Y.; Kuboki, T.; Takahashi, K.; Shinmura, T. J Mater Sci Lett 1997, 16, 1489.
24. Lazzeri, A.; Bucknall, C. B. J Mater Sci 1993, 28, 6799.
25. Yanchun, H.; Ralf, L.; Wolfgang, G. Die Angew Makromol Chem 1999, 270, 13.
26. Yanchun, H.; Ralf, L.; Wolfgang, G. J Appl Polym Sci 2000, 75, 1605.
27. Yanchun, H.; Ralf, L.; Wolfgang, G. J Appl Polym Sci 2001, 79, 9.